Numerical study of optimal trajectories with singular arcs for an Ariane 5 launcher

Pierre Martinon, J. Frederic Bonnans, Julien Laurent-Varin, Emmanuel Trélat

Numerical study of optimal trajectories with singular arcs for an Ariane 5 launcher

P. Martinon*
INRIA, 78153 Rocquencourt Cedex, France

F. Bonnans†
INRIA, 78153 Rocquencourt Cedex, France

J. Laurent-Varin‡
Centre National d'Etudes Spatiales, 91023 Evry Cedex, France

E. Trélat§
Université d'Orléans, 45067 Orléans Cedex 2, France

Introduction

We consider a flight mission to the geostationary transfer orbit (GTO) for an Ariane 5 launcher, while maximizing the payload or, as a variant, minimizing the fuel consumption. We first solve the complete flight sequence up to the final orbit, assuming a maximal thrust for all propulsion systems. Then we focus on the atmospheric ascent phase, which has been studied for instance in [1, 2, 3]. We are more specifically interested in optimal trajectories with singular arcs (flight phases with a non maximal thrust) for the boosters. Due to the presence of tabulated data in the physical model, the exact expression of the singular control cannot be obtained from the time derivatives of the switching function. An alternate way to compute the singular control is provided, and numerical experiments are carried out for for several launcher variants.

1 Problem statement

State and control variables

The state variables include the position and speed of the launcher, in dimension 3, as well as the masses of the three fuel-consuming parts of the launcher: m_1

*Research scientist, Team COMMANDS, INRIA-Saclay and Centre de Mathématiques Appliquées, Ecole Polytechnique, 91128 Palaiseau, France, Pierre.Martinon@inria.fr

†Senior research scientist, Team COMMANDS, INRIA-Saclay and Centre de Mathématiques Appliquées, Ecole Polytechnique, 91128 Palaiseau, France, Frederic.Bonnans@inria.fr

‡Engineer, Launchers Directorate, Rond-point de l'Espace, Evry, France, Julien.Laurent-Varin@cnes.fr

§Professor, Laboratoire MAPMO, UMR CNRS 6628, Fédération Denis Poisson, FR 2964, Bâtiment de Mathématiques BP 6759, Emmanuel.Trelat@univ-orleans.fr.

for the two boosters (treated as one propulsion system), m_2 for the first stage, and m_3 for the second stage (m denoting the total mass). This allows us to treat the separations more easily, avoiding the discontinuities on the state variables. Such discontinuities can be treated properly when applying Pontryagin's Minimum Principle (see for instance [4]), but in view of the disappointing numerical results, we got rid of discontinuities by splitting the total mass. The original problem being with free final time, we use the standard transformation to obtain a formulation with a fixed final time.

The control variables include the throttle $\alpha \in [0,1]$ for the boosters (we assume a maximal thrust for the propulsion systems of the stages), and the flight angles θ and ψ (heading and azimuth) giving the thrust direction. The control vector is then

$$u = (\alpha, \theta, \psi) \in [0,1] \times [-\pi, \pi]^2. \tag{1}$$

Flight dynamics

The dynamics for the masses correspond to the fuel consumption, which depends on the flight phase. The flight dynamics are

$$\begin{cases} \dot{r} = v \\ \dot{v} = \frac{1}{m}(T(r,u) - D(r,v)) \ + \ g(r) \\ \dot{m}_i = -\alpha \ \beta \quad \text{(for each fuel-consuming part)} \end{cases} \tag{2}$$

with
• $T(r,u) = \alpha \ \beta \ Isp \ g_0 \ - S \ P_z$: rocket thrust.
β : mass flow rate; Isp : specific impulse
S : area at rocket exit; P_z : atmospheric pressure (table)
• $D(r,v) = q \ Sr \ C_x(M)$: drag due to earth atmosphere.
q : dynamic pressure; S_r: reference area
C_x: drag coefficient (table); M : speed in Machs
• $g(r) = -\frac{\mu}{\|r\|^3} \ (r + J_2 \ \frac{R_T^2}{\|r\|^2} \ M_{J_2} \ r)$: gravity with J_2 corrector term.

Note: the lift term in the aerodynamic forces is here omitted.

Applying Pontryagin's Minimum Principle shows a decoupling for the control variables. Minimizing the Hamiltonian leads to the thrust direction being opposite to the speed costate, while the throttle follows a bang-bang law, with possible switchings or singular arcs.

Complete flight at full thrust

We start by solving the complete flight with stage separations, by setting a full thrust for the boosters. We want here to maximize the payload, and assume all fuel is burnt. As we consider the mass of each component instead of the global mass, the state variables remain continuous at the separations times. Therefore the separation times t_1 and t_2 for the boosters and first stage only need to satisfy the continuity of the Hamiltonian. We introduce as additional shooting unknowns the value of the state and costate at the separation times, namely, (x^1, p^1) and (x^2, p^2), for a better numerical behaviour. We have the

corresponding matching conditions that enforce the continuity of x and p at the separation times.

Numerical results

Solving the complete flight problem directly with the shooting method is difficult, due to the lack of a suitable initial guess. We first solve the flight restricted to the first phase (until separation of the boosters) then add the second and third phase. We obtain a solution with a payload of 14623kg and a final time of 1232.75 seconds. Boosters separation occurs after 119 seconds, and 533.375 seconds for the first stage, which is consistent with the constraints set on the final masses (consumption of all fuel).

Remark: The thrust is actually completely fixed during the first 10 seconds of the flight, vertical and maximal.

The first two graphs in Fig.1 represent the optimal control with the thrust level for the boosters and two stages, here set to 1, and the heading and azimuth angles for the thrust direction; and the masses of the different parts of the launcher. The separations correspond to the discontinuities observed on the total mass.

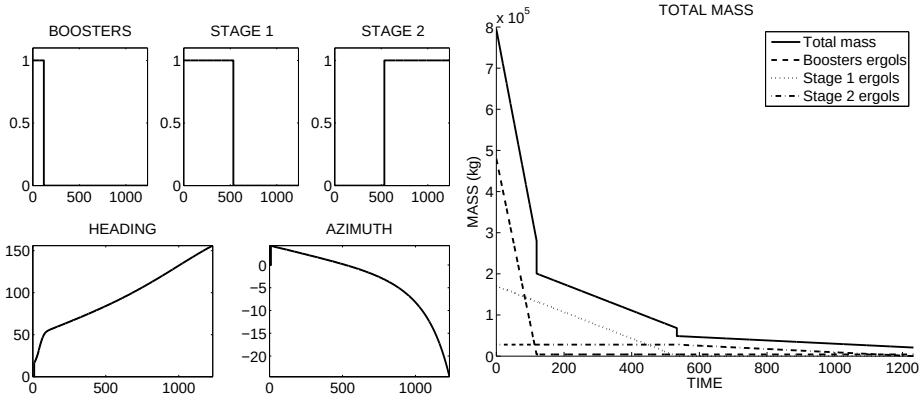

Fig.1 Complete flight with full thrust - Controls and masses

Fig.2 shows the evolution of the altitude and speed of the launcher during the flight. The change of the propulsion system at the beginning of the second and third phases is clearly visible on the speed graph. These graphs are consistent with the typical GTO flight described, for instance, in the Ariane 5 User's Manual from Arianespace.

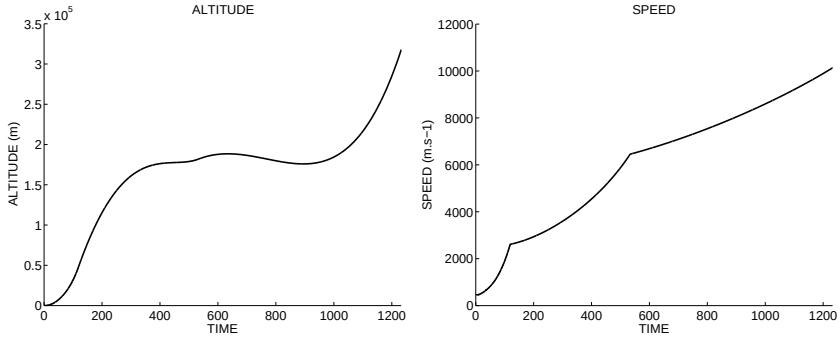

Fig.2 Complete flight with full thrust - Altitude and speed

Remark: It should be kept in mind that we have allowed a free direction for the thrust, which is not the case in the real flight where the thrust direction is strongly constrained by the dynamic pressure limit. However, the trajectory we obtained is close to the reference one.

2 Study of singular arcs for the boosters

We focus now on the study of singular arcs for the boosters, whose throttle is now free in $[0, 1]$, while keeping a maximal thrust for the two stages. We also restrict the flight to the first atmospheric climbing phase until the separation of the boosters. We reformulate the payload maximization criterion into a fuel consumption minimization, which is more suitable for the study of singular arcs. As we are only considering a variable throttle for the boosters (EAP), we set as the new criterion

$$Min \int_0^{t_f} \alpha \ \beta_{EAP}. \tag{3}$$

The payload is now fixed and is no longer part of the state variables, and the final masses m_1, m_2, m_3 are free. We also replace the final condition on the orbit by new final conditions on the position and speed. We take the values corresponding to the boosters' separation on the trajectory previously computed for the complete flight with full thrust.

2.1 An alternate expression for the singular control

A singular arc is characterized by the fact that the switching function ψ (the derivative of the Hamiltonian with respect to the control) vanishes over a whole time interval. The expression of the singular control is usually obtained by differentiating the equation $\psi(x, p) = 0$ with respect to time until the control appears explicitely (the required order of differentation being always even, see for instance [5]). However, due to the presence of tabulated data in the thrust and drag terms, the analytic expression of $\ddot{\psi}$ is already not available. We only have the first derivative $\dot{\psi}$ that depends on $\dot{x}$ and $\dot{p}$. As the idea behind the formal expression of the singular control is that the switching function and its successive time derivatives vanish over a singular arc, we try to enforce this constraint with the terms at our disposal.

Therefore, for the singular control we choose at each time step the value $\tilde{\alpha}_{sing}$ that minimizes ψ and $\dot{\psi}$ at the next integration step, i.e.,

$$\tilde{\alpha}_{sing} = ArgMin_{[0,1]} \|(\psi(y_{i+1}), \dot{\psi}(y_{i+1}))^t\|^2 \;=\; \psi^2(y_{i+1}) + \dot{\psi}^2(y_{i+1}), \qquad (4)$$

where y_{i+1} denotes the state-costate pair (x, p) obtained after one integration step from the current time. This minimization is currently performed by a BFGS method [6], starting from an initial value $\alpha = 0.5$. The numerical experiments showed that taking 0.1 or 0.9 as initial values gives similar results, which is of course reassuring. Furthermore, using the singular control continuity to initialize this minimization step (after the arc entry) seems to give slighltly better results than using a constant initialization.

We tested this formulation on the three dimensional Goddard problem (cf [7]) and found control values quite close to the exact value α^*_{sing} obtained from the equation $\ddot{\psi}(x, p) = 0$, see Fig.3. The difference between the exact singular control and the alternate formulation is about 10^{-3}, but the computational cost is significantly increased. However, the minimization procedure was not optimized and so might be further improved.

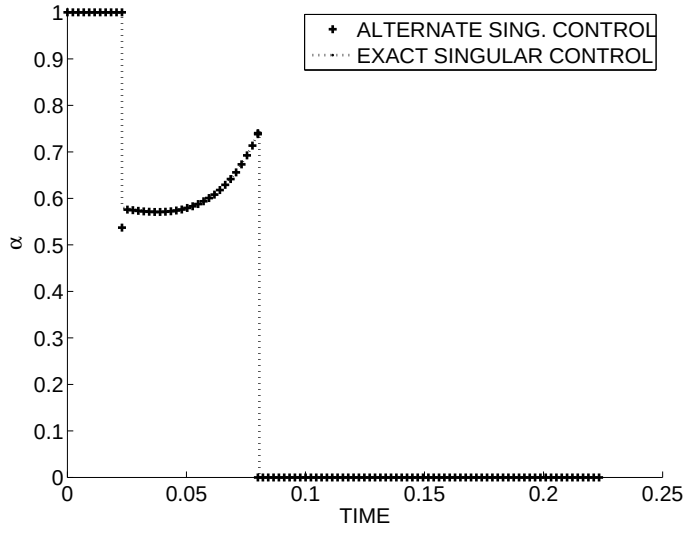

Fig.3 3D Goddard problem - Approximate and exact singular control

2.2 Continuation approach for singular arcs

In order to solve a problem with singular arcs, besides the expression of the singular control, we also need some information about the control structure, namely the number and position of the singular arcs. To obtain such information, we approach the original problem by a sequence of regularized problems with strictly convex Hamiltonians (with respect to the throttle), such as in [8, 7], for instance. This is done by adding a quadratic term to the criterion, which becomes, for given $\lambda \in [0, 1]$:

$$Min \int_0^{t_f} \left[\alpha\ \beta_{EAP} + (1-\lambda)\ \alpha^2 \beta_{EAP}\right] \mathrm{d}t. \qquad (5)$$

This regularization adds a new term $(1-\lambda)\ \alpha^2\beta_{EAP}$ to the Hamiltonian, which gives the modified command law for $\lambda < 1$:

$$\left\{\begin{array}{lll} If & \psi(x,p) > 0 & then \quad \alpha = 0 \\ If & \psi(x,p) < -2(1-\lambda)\beta_{EAP} & then \quad \alpha = 1 \\ If & -2(1-\lambda)\beta_{EAP} < \psi(x,p) < 0 & then \quad \alpha = \frac{-\psi(x,p)}{2(1-\lambda)\beta_{EAP}}. \end{array}\right. \tag{6}$$

The optimal control is now continuous, without singular arcs or switchings.

We perform a discrete continuation on this problem family, and solve an automated sequence of problems $(P)_\lambda$ starting from $\lambda = 0$. We use a very basic algorithm to generate the sequence of problems:
• Solve (P_0)
• Iterate: set $\lambda_{k+1} = \lambda_k + h$ and solve $(P_{\lambda_{k+1}})$ using (P_{λ_k}) as initialization, with a linear prediction ($h = 1$ initially, and is decreased in case of failure)
• Stop when reaching $\lambda = 1$, or maximum number of iterations / minimal step-size for h.

Notice that we do not actually need to reach $\lambda = 1$, but we still need to obtain sufficient information regarding the control structure, as well as a suitable initialization for the shooting method adapted to the singular structure.

However, even the strongly regularized problem (P_0) is not easy to solve directly, so we add a second layer of continuation over atmospheric forces, gradually introducing the atmospheric drag for the problem (P_0). Numerical experiments indicate that it is usually easy to solve the regularized problem in vacuum and complete the continuation on the drag, which gives a solution for the regularized problem (P_0). We can then begin the regularization homotopy in order to determine the control structure. The results of this method are described below, first for the original Ariane 5 launcher, and then for a slightly modified launcher.

Note: All numerical simulations were run on a standard desktop computer (Pentium IV 2.4GHz), using the gfortran compiler. Using a fixed-step RK4 integration (100 steps) and the HYBRD solver (see [9]) for the shooting method, the total cpu time for the atmosphere and regularization continuations and the final shooting is about 10 minutes.

2.3 Study of the original launcher

We first apply the approach described above to the original launcher problem, with a fixed payload $m_{CU} = 12610kg$. The regularized problem in vacuum can be solved from a very simple starting point: $(t_f = 100, p_r(0) = (-0.1, -0.1, 0.1)$, $p_v(0) = (-10^3, -10^3, -10^3)$ and $p_i(0) = -0.1, i = 1 \dots 3)$. The preliminary continuation is performed without any difficulties and gives a solution of (P_0). During the main continuation, we observe (see Fig.4) that the interval with a non-maximal thrust becomes smaller when the regularization decreases as λ tends to 1. At $\lambda = 0.999$, we have a solution with a full thrust throughout the flight except for the last few seconds, but with no sign of a singular arc.

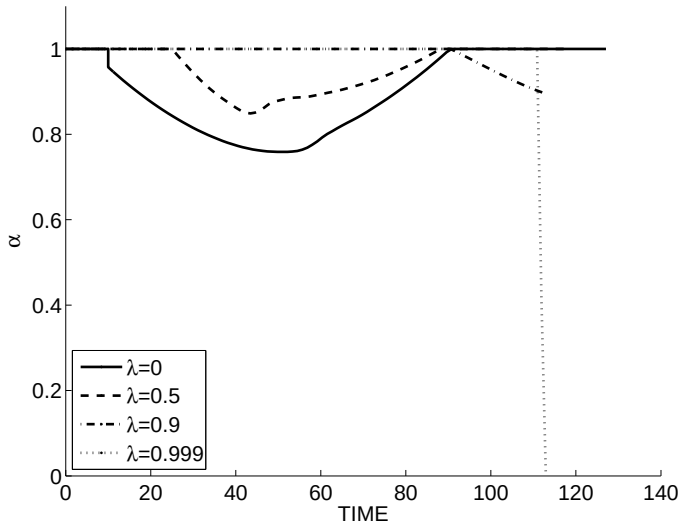

Fig.4 Regularization homotopy: thrust level for $\lambda = 0, 0.5, 0.9, 0.999$

We make some simple experiments with a direct method: piecewise constant control with 100 steps, RK4 integration for the state, IPOPT (see [10]) solver for the resulting optimization problem. We find a similar solution, with a full thrust and a switching to null thrust just before the end of the flight. Thus both methods suggest that the optimal solution to this problem does not present singular arcs.

2.4 Study of a modified launcher

Now we modify the launcher parameters in order to increase the drag effect: we increase the reference area S_r and the specific impulse Isp_{EAP}. For $S_r \times 2$ and $Isp_{EAP} \times 1.25$, we find an optimal trajectory with a singular arc.

As before, the regularized problem with no drag is easily solved, and the first continuation to introduce the drag poses no difficulties. Then we perform the regularization continuation until $\lambda = 0.95$, which shows strong hints of a singular arc. The graphs in Fig.5 show the thrust level and switching function at the solutions for $\lambda = 0$, 0.5, 0.9 and 0.95. Contrary to the previous case, we observe a small time interval (around $t = 30s$) where the thrust level remains in $]0, 1[$. Moreover, we see that the switching function ψ comes closer to 0 at the same time interval. These two facts together strongly suggest the presence of a singular arc. What happens at the end of the flight is less clear, as the thrust level again takes values in $]0, 1[$, and decreases near t_f. This could indicate a second singular arc, maybe followed by an arc with a null thrust, or just a switching to a null thrust arc.

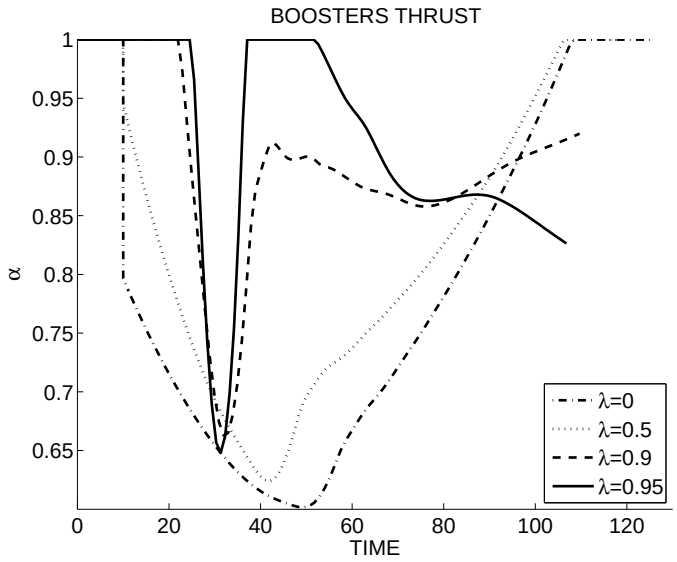

Fig.5 Regularization homotopy: thrust level for $\lambda = 0, 0.5, 0.9, 0.95$

The shooting method fails to converge for structures with two singular arcs, but the formulation with one arc actually gives a solution with a singular arc and a switching at the end. We detail below the shooting formulation for a control structure assuming one interior singular arc. In addition to the usual shooting unknowns (final time and initial costate), we have the entry and exit times for the singular arc. The corresponding additional conditions ensure that we enter the switching surface tangentially at t_{entry}, i.e. $\psi(x(t_{entry}), p(t_{entry}) = \dot{\psi}(x(t_{entry}), p(t_{entry})) = 0$, see for instance [4]. Notice that the switching at the end is handled automatically by a switching detection algorithm checking the sign of the switching function during the integration (see for instance [11], pages 195-200).

Shooting formulation for one interior singular arc

• **Shooting function unknown** $z \in \mathbf{R}^{12}$**:**

$$z = (t_f, p_r(0), p_v(0), p_m(0), t_{entry}, t_{exit}).$$

We use the solution from the end of the regularization continuation ($\lambda = 0.986$ after 100 iterations) to initialize z.

• **Shooting function value** $S(z) \in \mathbf{R}^{12}$**:**

$$\left\{ \begin{array}{ll} r(t_f) - r_f & \textit{Final position} \\ v(t_f) - v_f & \textit{Final speed} \\ p_{t_f}(t_f) & \textit{Final time TC} \\ p_{m_i}(t_f)\ , i = 1..3 & \textit{Final masses TC} \\ \psi(x(t_{entry}), p(t_{entry})) & \textit{Switching conditions} \\ \dot{\psi}(x(t_{entry}), p(t_{entry})) & \textit{at entry time} \end{array} \right. \tag{7}$$

Once again, we test a basic direct method, and find a similar solution. The graph on Fig.6 shows these results, with the small singular arc (about 2 seconds)

clearly visible on both solutions from the indirect and direct methods, around $t = 30s$. Both solutions also confirm that we have a simple switching near the end of the flight, and not a second singular arc.

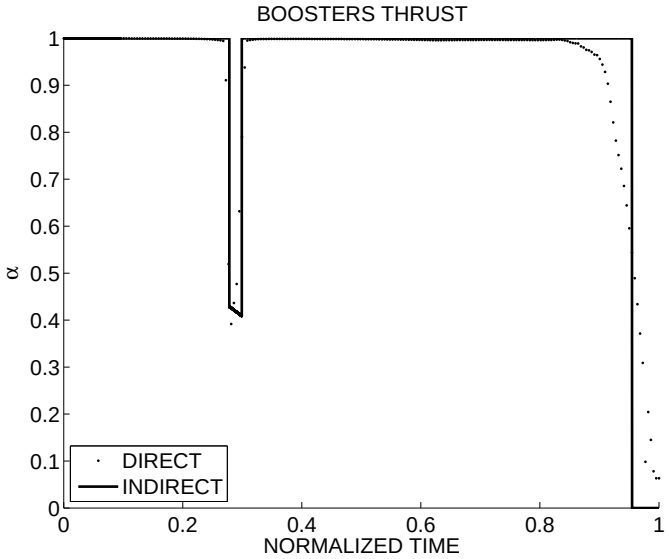

Fig.6 Solution with singular arc for $\lambda = 1$

As expected, the switching function ψ and its first derivative $\dot{\psi}$ are both close to 0 on the singular arc, around 10^{-3} and 10^{-4} respectively. Thus the approach of computing the singular control that minimizes $\psi^2 + \dot{\psi}^2$ worked rather well on this problem.

The criterion value (i.e., final mass of the EAP) is quite close for both solutions, with $m_1(t_f) = 165163kg$ for the shooting method and $m_1(t_f) = 164990kg$ for the direct method. Solving the same problem with the direct method with a fixed **bang(1)-bang(0)** control structure gives a close solution (without the singular arc of course), with a criterion of $m_1(t_f) = 164442kg$. It is comforting to observe that the solution with the singular arc is indeed slightly better than the forced bang-bang one, even if the difference is quite small.

It seems reasonable to assume that for a different set of parameters that would give a solution with a longer singular arc, the gain compared to the bang-bang solution would be more significant. Indeed, we can perform a continuation directly on the solution with a singular arc and further increase the value of the parameter S_r. We observe that the solutions exhibit longer singular arcs when S_r increases, with a more significant gain with respect to the corresponding solution (Fig.7).

	$S_r \times 2$	$S_r \times 2.5$	$S_r \times 3$
$m_1(t_f)$ (singular arc)	165163 kg	160199 kg	155986 kg
$m_1(t_f)$ (bang-bang)	164442 kg	159172 kg	154202 kg
Arc duration	2.1 sec	9.4 sec	15.3 sec
Mass gain	721 kg	1027 kg	1784 kg

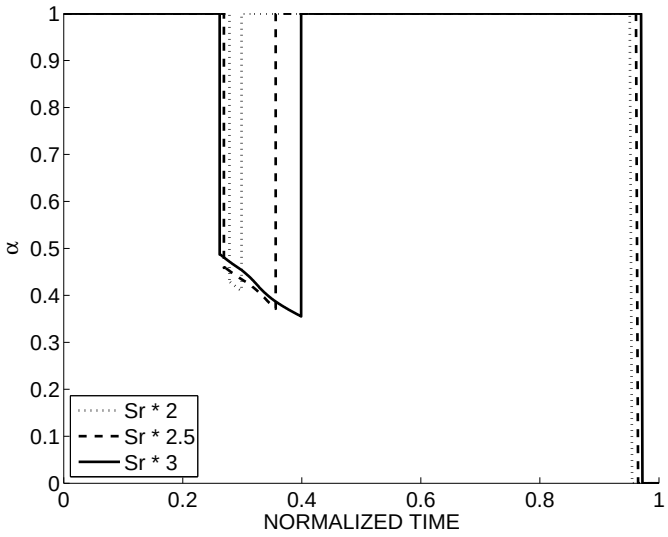

Fig.7 Singular arcs for increasing values of S_r

Conclusion

This study indicates that while the original problem for an Ariane 5 launcher seems to admit a simple bang-bang optimal solution, slightly modifying some parameters such as the reference area and specific impulse of the launcher gives an optimal solution with a singular arc. We also introduced a new way of computing the singular control when its analytic expression from the time derivatives of the switching function is not available (here due to the presence of tabulated data in the physical model). We plan to extend this work to the study of a winged launcher while taking into account the lift force and dynamic pressure constraint.

Acknowledgement

This study was supported by Centre National d'Etudes Spatiales, Paris.

References

[1] Seywald, H., and Cliff, E.M., "Goddard problem in presence of a dynamic pressure limit", *Journal of Guidance, Control, and Dynamics*, Vol. 16, No. 4, pp. 776-781, 1993.

[2] Calise, A.J., and Gath, P.F., "Optimization of launch vehicle ascent trajectories with path constraints and coast arcs", *Journal of Guidance, Control, and Dynamics*, Vol. 24, No. 2, pp. 296-304, 2001.

[3] Lu, P., Sun, H., and Tsai, B., "Closed-loop endoatmospheric ascent guidance", *Journal of Guidance, Control, and Dynamics*, Vol. 26, No. 2, pp. 283-294, 2003.

[4] Pesch, H.J., "A practical guide to the solution of real-life optimal control problems", *Control and Cybernetics*, Vol. 23, pp. 7-60, 1994.

[5] Robbins, H.M., "A generalized Legendre-Clebsch condition for the singular case of optimal control", *IBM J. of Research and Development*, Vol. 11, pp. 361-372, 1967.

[6] Byrd, R.H., Lu, P., Nocedal, J., and Zhu, C.Y., "A limited memory algorithm for bound constrained optimization", *SIAM J. Sci. Comput.*, Vol. 16, No. 5, pp. 1190-1208, 1995.

[7] Bonnans, F., Martinon, P., and Trélat, E., "Singular arcs in the generalized Goddard's problem", *Journal of Optimization Theory and Applications*, Vol. 138, No. 2, 2008. to appear in august 2008.

[8] Gergaud, J., and Martinon, P., "An application of PL continuation methods to singular arcs problems", In A. Seeger, editor, *Recent Advances in Optimization*, Volume 563 of *Lectures Notes in Economics and Mathematical Systems*, pp. 163-186. Springer-Verlag, 2006.

[9] Garbow, B.S., Hillstrom, K.E., and More, J.J., "User Guide for Minpack-1", National Argonne Laboratory, Illinois, 1980.

[10] Waechter, A., and Biegler, L.T., "On the implementation of an interior-point filter line-search algorithm for large-scale nonlinear programming", *Mathematical Programming Series A*, Vol. 106, pp. 25-57, 2006.

[11] Hairer, E., Nørsett, S.P., and Wanner, G., "Dense output, discontinuities, derivatives", *Solving ordinary differential equations. I*, volume 8 of *Springer Series in Computational Mathematics*. Springer-Verlag, Berlin, 1993, pp 195-200.